Separation Science and Technology
Publication details, including instructions for authors and subscription information:
http://www.informaworld.com/smpp/title~content=t713708471

Multicomponent Fixed-Bed Ion Exchange: Verification of Equilibrium Coherence Theory

Carol B. Bailey[a]; Neville G. Pinto[a]
[a] Department of Chemical and Nuclear Engineering Mail Location 171, University of Cincinnati, Cincinnati, OH

To cite this Article Bailey, Carol B. and Pinto, Neville G.(1988) 'Multicomponent Fixed-Bed Ion Exchange: Verification of Equilibrium Coherence Theory', Separation Science and Technology, 23: 12, 1853 — 1873
To link to this Article: DOI: 10.1080/01496398808075668
URL: http://dx.doi.org/10.1080/01496398808075668

SEPARATION SCIENCE AND TECHNOLOGY, 23(12&13), pp. 1853-1873, 1988

MULTICOMPONENT FIXED-BED ION EXCHANGE: VERIFICATION OF EQUILIBRIUM COHERENCE THEORY

Carol B. Bailey
Neville G. Pinto
Department of Chemical and Nuclear Engineering
Mail Location 171
University of Cincinnati
Cincinnati, OH 45221-0171

ABSTRACT

The coherence method, a technique for modeling multicomponent fixed-bed adsorption with time dependent feed conditions, has been applied to a fixed-bed ion-exchange system under a variety of operating conditions. Theoretically, the method can handle multicomponent systems with initial and feed conditions of any degree of complexity. This paper will present the results of an experimental study to verify the practical utility of the coherence method. A ternary ion-exchange system of K^+, Na^+, Li^+ on a fixed bed of AG-50WX8 resin has been studied. Breakthrough curves have been obtained for single abrupt, multiple abrupt, and linear influent composition changes. A non-equilibrium model has also been developed and has been used to describe limiting binary exchange cases. The experimental breakthrough curves have been compared with the predictions of both models.

INTRODUCTION

A great deal of effort has been devoted to the study of adsorption and ion-exchange in fixed-bed systems. The standard approach has been to apply the equilibrium theory to locate constant composition zones (plateaus) and varying composition zones (transitions). Non-equilibrium effects are incorporated by formulating empirical rules to cover observed results. This approach is restricted to single component non-stoichiometric and binary stoichiometric systems (1). Furthermore, this method is practical only for constant feed conditions. For multicomponent systems or variable feed conditions, breakthrough curve predictions become much more complex due to interferences between transition zones.

A useful theory for predicting the behavior of multicomponent ion-exchange systems with significant interactions is the coherence theory developed by Helfferich and Klein (2). This equilibrium theory is applicable to multicomponent systems of virtually any degree of complexity. The theory has been applied to a variety of processes (3-9). In each case, good engineering approximations of breakthrough curves were obtained. It has been confirmed in all these studies that the mass-transfer limitation of the theory has only a secondary effect in that the experimental breakthrough curves are less abrupt than predicted.

The coherence theory has not yet been verified for multicomponent systems having variable influent conditions. One important practical example of variable influent conditions is gradient elution used in the separation of fission product rare earths (10). This chromatagraphic technique suppresses the excessive tailing of peaks produced when separating a relatively large number of similiar substances, permitting more efficient column utilization.

A physical non-equilibrium model for evaluating the kinetic behavior of multicomponent ion-exchange systems has also been presented. This model utilizes the Stefan-Maxwell relations of non-equilibrium thermodynamics and incorporates concentration dependent mass transfer coefficients for a prediction of multicomponent ion-exchange behavior.

The purpose of this investigation is to evaluate the effectiveness of both the coherence method and the non-equilibrium model. The non-equilibrium model was used to study binary separations of systems with favorable and non-favorable equilibrium conditions. The coherence model was applied to ternary exchange with single and multiple abrupt influent changes and also linear influent changes.

MULTICOMPONENT INTERFERENCE THEORY

The concentration profile or concentration history of a fixed-bed ion-exchange column can be predicted using the concentration velocities of all the mobile species in the column. For a given species i, the concentration velocity can be written as (11):

$$v_{c_i} = \left(\frac{\partial z}{\partial t}\right)_{c_i} = \frac{u_o}{1 + \left(\frac{\partial \bar{c}_i}{\partial c_i}\right)_z} \qquad i=1,.....,n \tag{1}$$

Adjusted concentration velocities, u_{x_i} and u_{y_i}, can be written in terms of normalized concentrations

$$x_i = \frac{c_i}{c} \tag{2}$$

$$y_i = \frac{\bar{c}_i}{\bar{c}} \tag{3}$$

and adjusted time

$$\tau = \frac{c\, u_o}{\bar{c}} \left(t - \frac{z}{u_o}\right) \tag{4}$$

in the following manner:

$$u_{x_i} = \left(\frac{\partial z}{\partial \tau}\right)_{x_i} \tag{5}$$

$$u_{y_i} = \left(\frac{\partial z}{\partial \tau}\right)_{y_i} \tag{6}$$

The adjusted velocities u_{x_i} and u_{y_i} are related to the true velocities by

$$v = \frac{u_o}{1 + \frac{\bar{c}}{cu}} \tag{7}$$

A key concept of the multicomponent coherence theory is that of "coherence". Coherence is characterized by the fact that at any given point and time in the column the concentration velocities of all species are equal;

$$u_{x_i} = u_{x_j} = u \qquad \text{for all } i \text{ and } j \tag{8}$$

This condition requires that the compositions within a coherent boundary be preserved.

As Helfferich has stated, "coherence is a state which any system strives to attain from arbitrary starting conditions" (2). Thus, concentration variations occuring in a coherent boundary must follow invariant composition paths. For situations with constant separation factors, these composition paths are linear.

Using the condition of coherence, modes which dynamic systems strive to attain can be identified independent of operating conditions. This phenomenon leads to a fairly simple and concise representation of column behavior.

For the case of constant separation factors, a mathematical transformation called the "h transformation" (2) can be used to orthogonalize the composition path grids. Using the h transformation, one can obtain the effluent composition history without solving a set of coupled partial differential equations. In addition, because of the orthogonal nature of the h space, only a single h value can change across a boundary (or wave) whereas concentrations of all species may change across the boundary. This greatly simplifies the calculations of the concentration velocities and zone compositions. The non-trivial roots of the new composition variable, h, can be calculated from either of the following equations:

$$\sum_i \frac{x_i}{(h-\alpha_{1i})} = 0 \tag{9}$$

$$\sum_i \frac{y_i}{\left(\frac{1}{h} - \alpha_{i1}\right)} = 0 \tag{10}$$

where the sums are taken over all exchanging species.

Once the roots have been established, the corresponding x_i and y_i can be calculated from:

$$x_i = \prod_j^{n-1} (h_j - \alpha_{1i}) \Big/ \prod_{j\neq i}^{n} (\alpha_{1j} - \alpha_{1i}) \tag{11}$$

$$y_i = \prod_j^{n-1} \left(\frac{1}{h_j} - \alpha_{i1}\right) \Big/ \prod_{j\neq i}^{n} (\alpha_{j1} - \alpha_{i1}) \tag{12}$$

The composition or wave velocity defined for coherent boundaries in terms of the h roots is:

$$v_{h_k} = h_k \prod_{i}^{n-1} h_i \prod_{i}^{n} \alpha_{il} \tag{13}$$

where h_k is the variable root.

The advantage of the coherence concept becomes more apparent for systems having variable initial or feed conditions. In these situations, boundaries traveling at different rates can interfere with one another producing a noncoherent wave. The basic rules governing the dynamic behavior of the h roots remain valid for interference. The noncoherent wave will be resolved into coherent waves with a constant composition zone between each wave.

For the situation of time dependent composition variations in the initial or feed conditions, the noncoherence persists over a finite distance-time region. In the noncoherent boundary, the various species concentrations at any fixed location and time advance at different rates, so that given compositions exist only momentarily. Thus, the individual behavior of all species must be considered, which means a quantitative description of composition histories requires numerical techniques. The pertinent simultaneous differential equations in terms of h roots are:

$$\left(\frac{\partial h_k}{\partial \tau}\right)_z = -h_k \prod_{i=1}^{n-1} h_i \prod_{i=1}^{n} \alpha_{il} \left(\frac{\partial h_k}{\partial z}\right)_\tau \qquad k=1,..,n \tag{14}$$

NON-EQUILIBRIUM MODEL

If the ion-exchange process occurred instantaneously, column performance could be accurately predicted from equilibrium theory, and, for favorable equilibrium in the absence of axial dispersion, the breakthrough curve would be ideally sharp. In general, it is necessary to consider the kinetics of the ion-exchange process for an accurate prediction of the breakthrough curve.

For particle phase mass-transfer control, the continuity equation applied to a single resin particle can be written as:

$$\left(\frac{\partial y_i}{\partial t}\right) + \nabla \cdot J_i = 0 \tag{15}$$

This equation can be integrated over a closed volume using Gauss' divergence theorem;

$$\left(\frac{\partial y_i}{\partial t}\right)_v = \frac{-a_p}{\bar{c}} \, n \cdot J_i \Big|_I \tag{16}$$

where a_p is the outer surface interfacial area of the sorbent particles per unit volume of contacting system.

Generally, the diffusion coefficient associated with the flux term is considered invariant with respect to composition; a premise that is not always justified. Pinto and Graham (12) have proposed a model for transport in multicomponent ion exchange which utilizes the Stefan-Maxwell relations:

$$(-y_i \nabla \mu_i') = \left(\frac{RT}{c}\right)\left(\frac{y_s J_i}{a_{is}\tau} + \sum_{j=1}^{n} \frac{y_j J_i - y_i J_j}{a_{ij}\tau} + \frac{y_f J_i}{a_{if}}\right) \qquad i=1,\ldots,n \tag{17}$$

The terms a_{is}, a_{ij} and a_{if} are the ion-solvent, ion-ion and the ion-fixed-site Stefan-Maxwell interaction coefficients, respectively, and are dependent on resin composition and total concentration. The term τ is the geometrical tortuosity factor and can be related to fractional pore volume using one of several theoretical models (13). It should be noted that in writing equation 17 it has been assumed that solvent flux is negligible.

The Stefan-Maxwell equations can be written in matrix form and inverted to give diffusional fluxes in terms of electrochemical gradients;

$$[J] = \frac{\hat{c}}{RT}[A]^{-1}[y \nabla \mu'] \tag{18}$$

The elements of the matrix [A] are a function of the Stefan-Maxwell coefficients, the composition, and the tortuosity factor. The Stefan-Maxwell equations in this form can be introduced into the continuity equation (eq. 15). The electrochemical potential is given by:

$$\mu_i' = \mu_i + z_i f \phi \tag{19}$$

and the electrical potential term, ϕ, in this equation (eq. 19) can be eliminated by using the no current condition

$$\sum_{i=1}^{n+1} z_i J_i = 0 \tag{20}$$

In equation 20, the no current condition has been applied to n counterion species and the fixed site.

The chemical potential term can be expressed in terms of concentration by assuming activity coefficient gradients are absent;

$$\nabla\mu_i = \frac{RT}{y_i}\nabla y_i \tag{21}$$

Glueckauf and Coates' (14) linear driving force approximation can be used to obtain an approximate representation of the concentration gradient. For particle phase control, the concentration of the fluid phase is assumed uniform throughout and up to the particle surface where it is in equilibrium with the resin. Within the particle, the concentration decreases linearly through an imaginary film to the average concentration in the particle. Thus,

$$u\cdot\nabla y_i\big|_I = \frac{y_i - y_i^*}{\delta} \tag{22}$$

where δ is the film thickness.

The following relationship is obtained for the continuity equation when equations 16-22 are substituted into equation 15:

$$\left(\frac{\partial y_i}{\partial t}\right)_\upsilon = \frac{-a_p \hat{c}}{\bar{c}\,\delta}\sum_{j=1}^{n+1} B_{ij}(y_j - y_j^*) \tag{23}$$

where B_{ij} are the elements of the inverse matrix in equation 18.

For the ion-exchange process neglecting longitudinal effects and Donnan uptake and assuming one dimensional plug flow, the differential column material balance can be written as:

$$F\left(\frac{\partial x_i}{\partial \upsilon}\right)_t + \frac{\bar{c}}{c}\left(\frac{\partial y_i}{\partial t}\right)_\upsilon + \varepsilon\left(\frac{\partial x_i}{\partial t}\right)_\upsilon = 0 \tag{24}$$

A dimensionless throughput parameter θ, which measures the ratio of the volume of the fluid that has passed to the volume of the contained adsorbent, can be defined as:

$$\theta = \frac{c\,(V-\varepsilon\upsilon)}{\bar{c}\,\upsilon} \tag{25}$$

which simplifies equation 24 to

$$-\left(\frac{\partial x_i}{\partial \upsilon}\right)_{\theta\upsilon} = \left(\frac{\partial y_i}{\partial \theta\upsilon}\right)_\upsilon \tag{26}$$

The hyperbolic nature of this system allows numerical integration of the partial differential equations separately along two families of characteristic curves: that of constant υ and that of constant $\theta\upsilon$. Thus, equation 26 can be separated into two equations.

$$(\partial x_i/\partial \upsilon)_{\theta\upsilon} = -R_i \tag{27}$$

$$(\partial y_i/\partial \theta\upsilon)_{\upsilon} = R_i \tag{28}$$

where R_i can be determined using the appropriate rate equation (eq. 23).[1]

A simultaneous solution of the rate expression and the column material balance will generate a description of the ion-exchange behavior, provided the boundary and the initial conditions are known.

EXPERMENTAL METHODS

Experimental studies were performed using a small scale ion-exchange column to determine both column breakthrough behavior and equilibrium characteristics of the resin. The ternary exchange of potassium, lithium, and sodium on AG 50W-X8 ion-exchange resin was investigated using 1.0 M total concentration to ensure particle diffusion control. Chloride was the co-ion in each case. AG 50W-X8 is a strongly acidic cation exchange resin of a sulfonated polystyrene with 8% divinylbenzene crosslinking. The commercial resin in the H-form has 65-115 wet mesh size and an average diameter of approximately 0.18 mm. The selectivity sequence for this resin is K>Na>Li.

Equilibrium properties of the resin such as water content, size, and resin density were determined at various solution compositions and 1.0 M total concentration. The resin was equilibrated in a shallow bed containing approximately 5 g of resin. A sufficient volume of equilibrating solution was fed at a dropwise flow rate to guarantee complete conversion. Once equilibrated, the resin was washed with deionized water. Resin density measurements were performed in a 10 ml specific gravity bottle. The mean diameter was determined from a statistical sampling of the equilibrated resin using a moving-vernier-scale microscope. Internal water content was estimated using the method described by Scatchard and Anderson (15).

Figure 1 is a schematic depicting the apparatus used for the kinetic measurements.

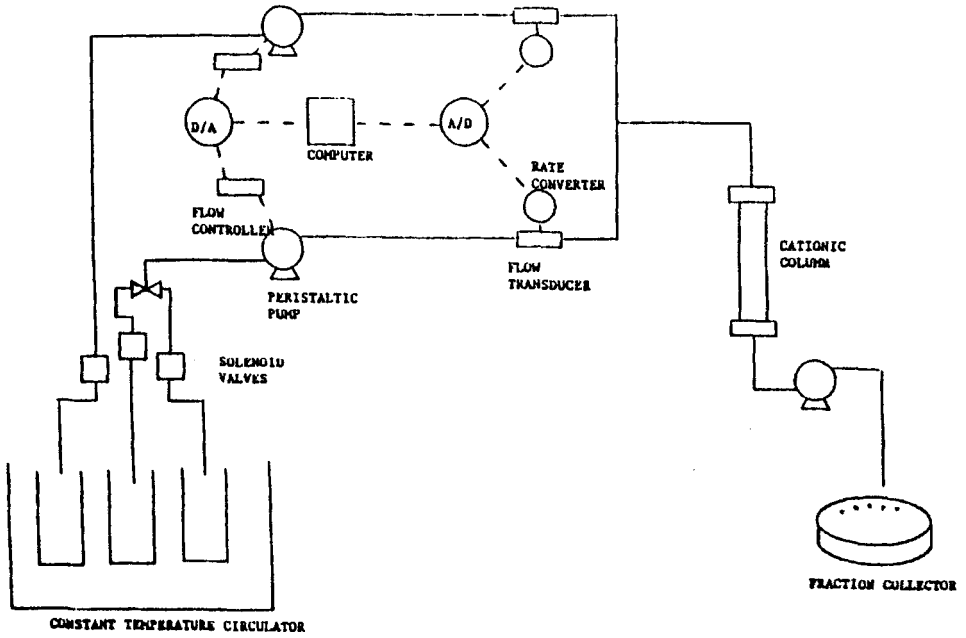

Figure 1. Experimental Apparatus for Determining Effluent Concentration Histories

The resin bed was contained in a glass tube of 25 mm i.d. The total bed height was approximately 40 cm. A constant temperature bath provided a feed solution at $25 \pm 0.2^{0}C$. The solution was fed to the column at a constant total flow rate using peristaltic constant velocity pumps. The kinetic studies were performed under conditions of single and multiple abrupt influent composition changes and also linear influent composition changes. Multiple abrupt influent changes were obtained by switching feed compositions using a manifold of solenoid valves. The linear influent change was accomplished using computer aided feed back control of the flows. Two compositions were pumped simultaneously to the column, one with linearly increasing flow the other linearly decreasing, maintaining a constant total flow to the column.

Equal effluent volumes were collected by an automatic fraction collector. Cationic concentrations were determined using an inductively coupled plasma-atomic emission spectrometer (ICP-AES). The effluent concentration history of each species was established by monitoring the effluent of the column with time.

Table 1. Experimental Operating Conditions for Fixed-Bed Column

Run No.	Flow Rate (ml/min)	Bed Capacity (meq)	Type of Injection
1	11.0	582.6	Single abrupt
2	9.0	537.4	Double abrupt
3	26.5	560.8	Linear
4	9.0	560.8	Linear
5	10.0	542.3	Single abrupt
6	11.4	542.3	Single abrupt

Solution Concentration = 1.0 M

RESULTS AND DISCUSSION

Representative experimental effluent concentration histories for the ternary exchange system with various influent composition changes are displayed in Figures 2 and 4-8. Injection sequences are also reported in these figures. Table 1 lists column operating conditions and inlet conditions for each of the runs. In each situation, a constant initial column composition was used.

Predicted concentration histories were calculated from the coherence technique and are also portrayed in Figures 2 and 4-8. Normalized concentration velocities were determined from h roots and separation factors using equation 13. The assumption of constant separation factors was made, and is generally valid for ion-exchange systems. Separation factors were estimated as best-fit parameters from the observed effluent concentration histories of limiting binary exchange systems, and were then used in the prediction of other effluent concentration histories. The best-fit values were 1.25 and 2.0 for the K-Na system and the K-Li system, respectively. Average resin capacities were determined for each column run using correlations established from the equilibrium experiments. Column void fraction was determined as a best-fit parameter using several column runs with abrupt influent changes.

As Figure 2 indicates, the coherence technique accurately predicts the location and compositions of zones of varying and constant composition for single, abrupt influent changes. For

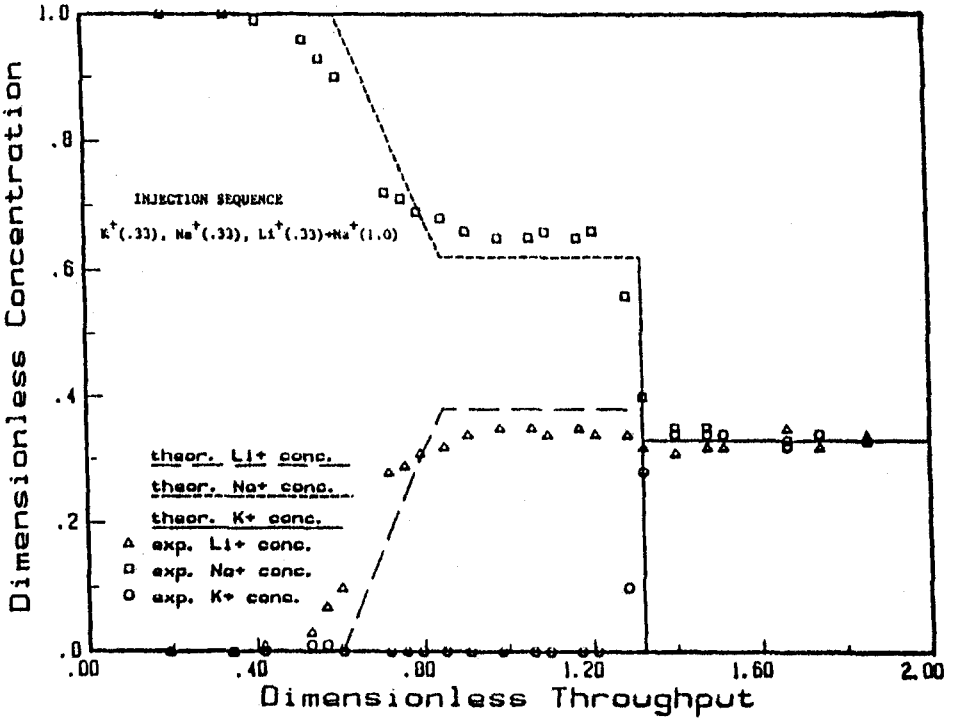

Figure 2. Effluent Concentration History for Run 1

example, the the existence of the diffuse wave followed by the plateau and finally the sharp breakthrough is accurately reflected by the theory.

The rules derived from the coherence method can also be applied to multiple, abrupt influent changes. Run 2 involves an injection generating a diffuse boundary followed by a second injection generating a self-sharpening boundary. The outcome of interferences resulting from multiple inputs is more easily understood using a distance-time diagram.

Figure 3 is the distance-time plot associated with Run 2. The self-sharpening and nonsharpening boundaries generated at the inlet have the same variable root and will merge to form a Na pulse. The intermediate Li zone disappears. From Figure 4 it is clear that the coherence theory predicts all the main features of

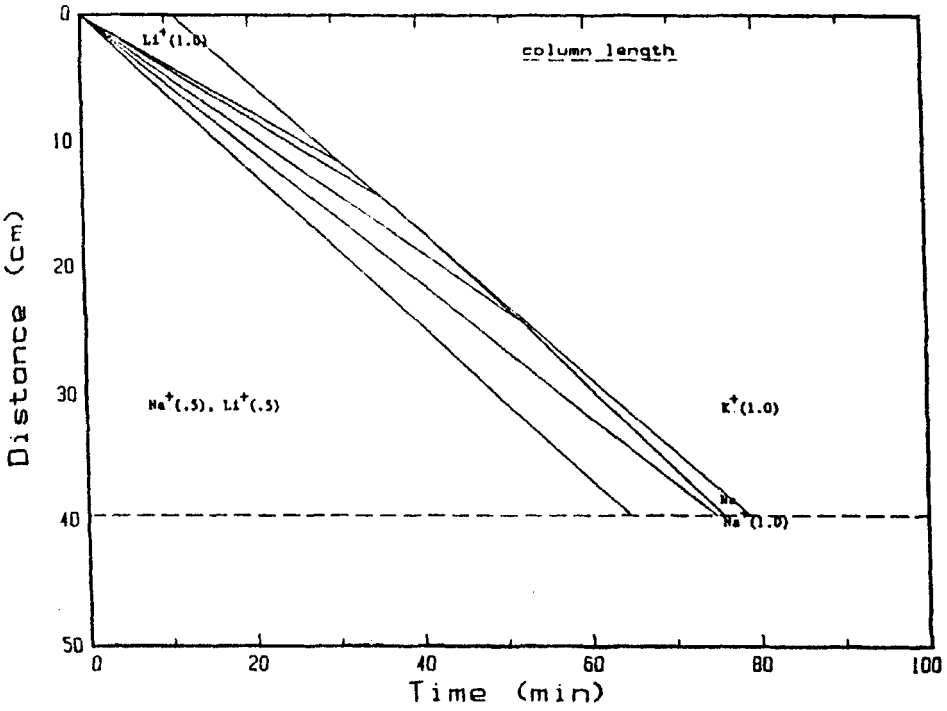

Figure 3. Distance-Time Diagram for Run 2

the double injection effluent concentration history. However, the necessity for the development of non-equilibrium models is also evident; diffusive resistances and dispersion effects significantly alter the effluent concentration histories. For example, in Figure 4 no pure Na pulse is obtained.

The linear influent composition change produces noncoherent boundaries which require finite distance and time for resolution into coherent boundaries. A quantitative description of the behavior of the noncoherent boundaries is obtained through a finite difference numerical solution of the coupled partial differential equations (eq. 14).

Self-sharpening boundaries were generated by a gradual influent composition change in Runs 3 and 4. Run 3 was performed with a linear composition change over a period of 25 minutes,

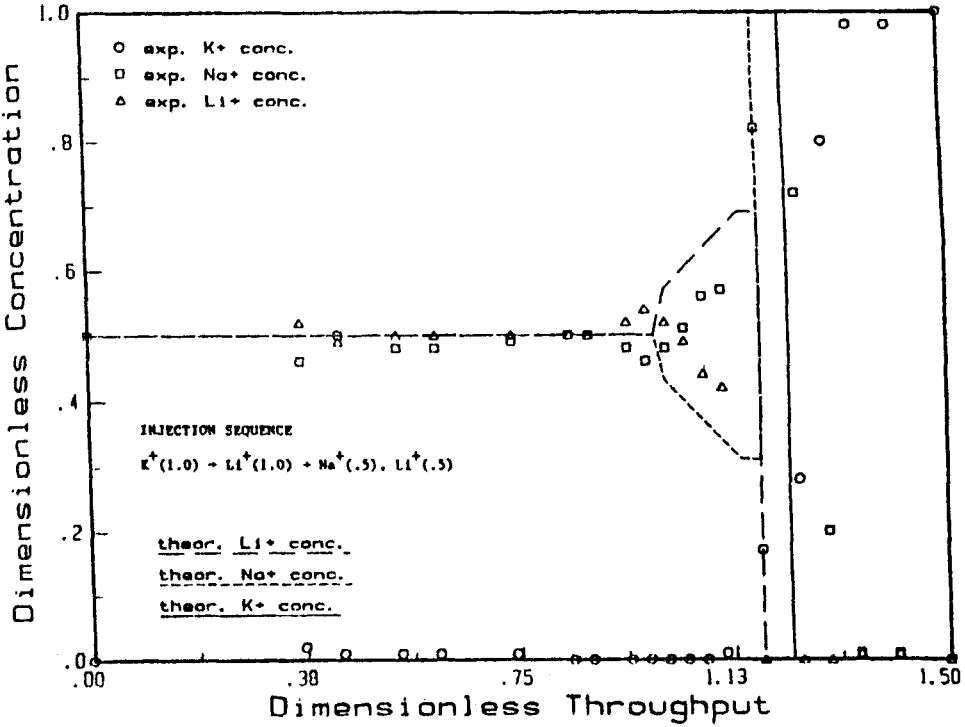

Figure 4. Effluent Concentration History for Run 2

whereas in Run 4 the same change was effected over a period of 10 minutes. In both these runs, column lengths were such that sufficient time was not allowed for resolution to the final pattern; therefore, the noncoherent region is observed in the final breakthrough. Figures 5 and 6 are the breakthrough curves associated with these runs. The coherence theory closely predicts the effluent concentration histories. Both curves indicate a tendency toward the final resolution pattern which contains a Na peak. Run 4 having the shorter time dependent period is closer to attainment of the final pattern.

The non-equilibrium model for fixed-bed ion exchange was applied to binary exchange systems. The mathematical prediction

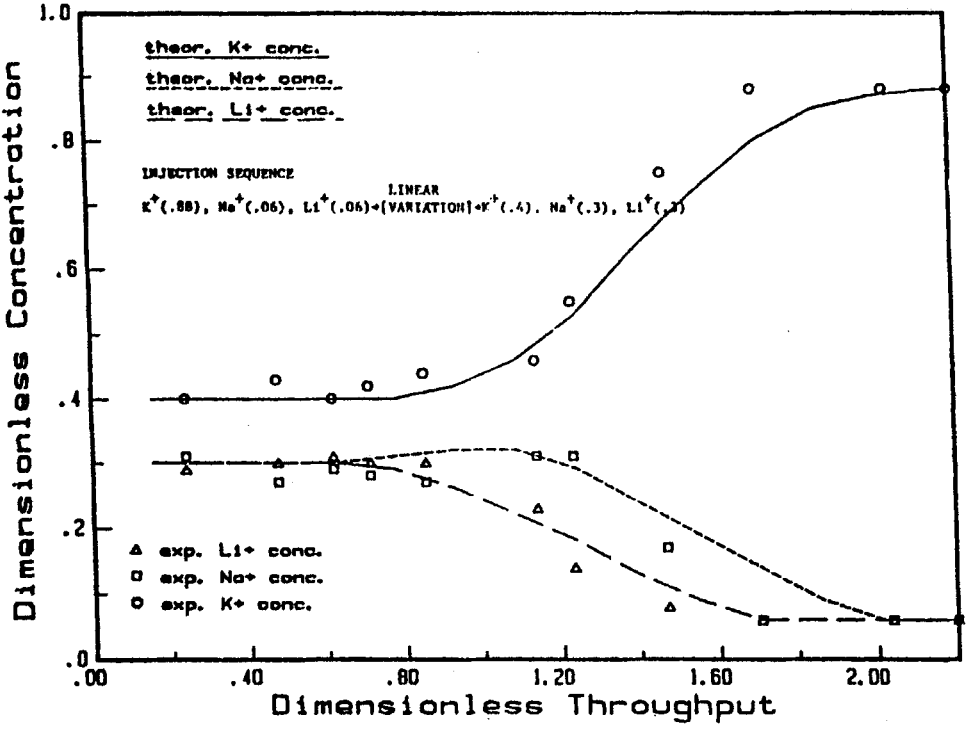

Figure 5. Effluent Concentration History for Run 3

of effluent concentration histories was obtained using the method of characteristics which involves simultaneous solution of the column material balance (eq. 26) and the rate equation (eq. 23) along a characteristic path grid.

The application of this model to ion exchange requires the calculation of the interaction coefficients, the tortuosity factor, and particle film thickness.

The interaction coefficients in equation 17, and consequently equation 23, have been related to fundamental physical properties

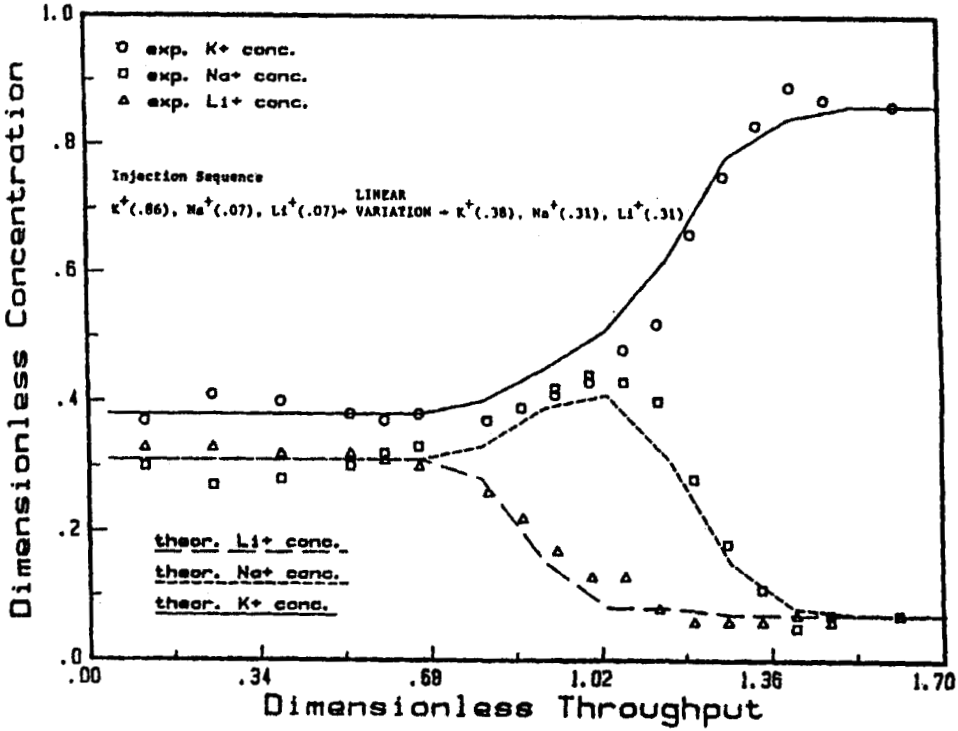

Figure 6. Effluent Concentration History for Run 4

of the resin (16):

$$a_{is} = kT\omega_i^{\circ}\,\bar{y}_s(\eta^{\circ}/\eta)^{0.7} \tag{29}$$

$$a_{ij} = \left[\frac{-2kT\omega_i^{\circ}\omega_j^{\circ}}{\omega_i^{\circ}|z_i| + \omega_j^{\circ}|z_j|}\right] g_{ij}(\bar{y}_{ij})^{2/3}\,(\eta^{\circ}/\eta)^{0.7} \tag{30}$$

$$a_{if} = kT\,\omega_i^{\circ}\,g_{if}\,(\bar{y}_{if})^{2/3}\,(\eta^{\circ}/\eta)^{0.7} \tag{31}$$

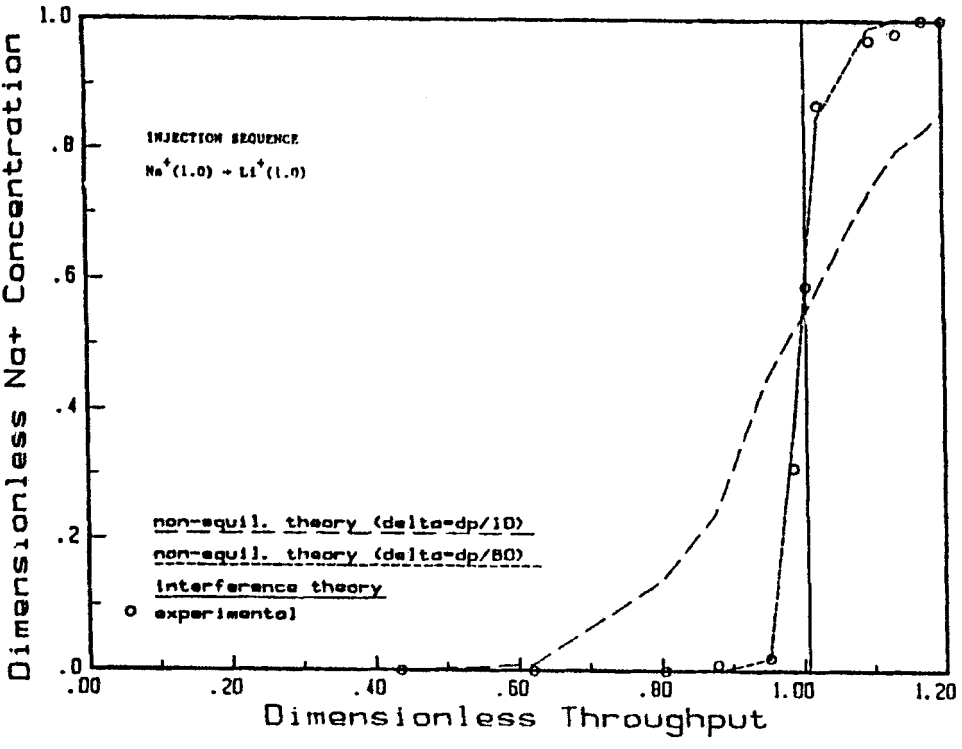

Figure 7. Effluent Concentration History for Run 5

The g_{ij} were obtained previously through the correlation of tracer diffusion data (16). The reported values are:

$$g_{NaLi}=2.46,\ g_{Naf}=0.063,\ \text{and}\ g_{Lif}=0.041\ .$$

The Stefan-Maxwell equations also include a tortuosity term which accounts for the physical obstruction by the matrix. Pinto and Graham (16) have shown that the Millington(13) model, $T=\varepsilon_p^{4/3}$, appears to best describe the tortuosity term for ion exchange, when used in conjunction with the Stefan-Maxwell model.

For situations in which the diffusivity is independent of concentration, the following semi-empirical expression provides a

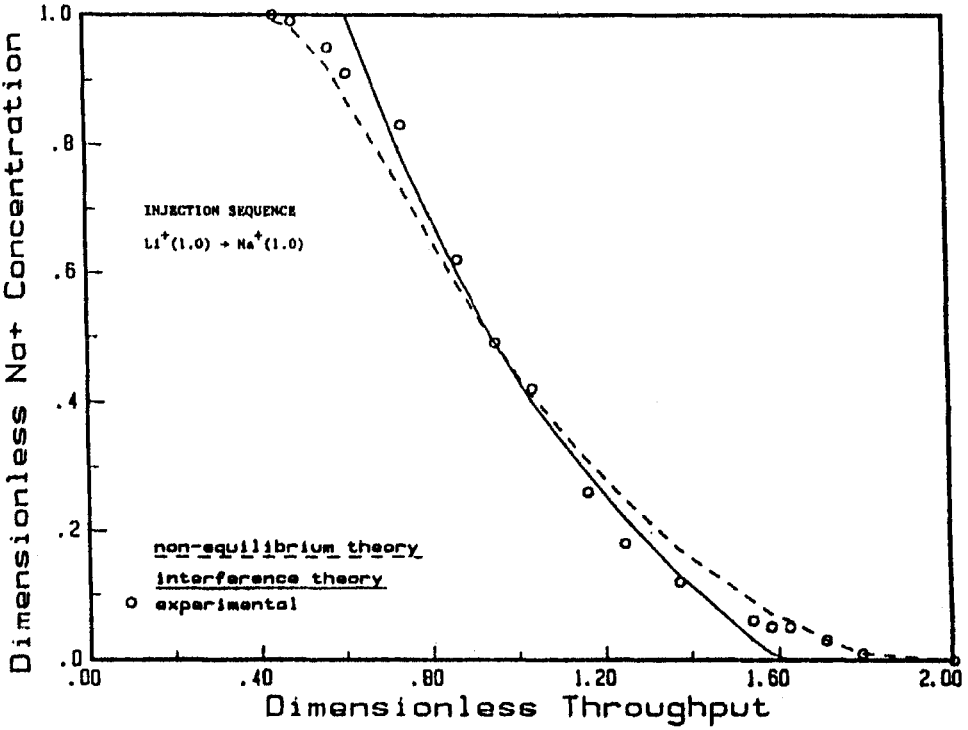

Figure 8. Effluent Concentration History for Run 6

good approximation for film thickness: $\delta=dp/10$ (14). However, since the Stefan-Maxwell equations involve concentration dependent diffusivities, it is unlikely that this expression will appropriately estimate film thickness.

The non-equilibrium model was applied to binary exchange systems with favorable and non-favorable equilibrium. Experimental and predicted breakthroughs are shown for Na^+/Li^+ and Li^+/Na^+ exchange in Figures 7 and 8, respectively. The solid lines represent breakthroughs predicted using the equilibrium coherence technique. The broken lines represent predictions based on the non-equilibrium model. Two film thicknesses were used for the predictions. It was found that the correlation of Glueckauf and Coates estimated too large a film thickness. A single breakthrough curve (Fig. 7) was used to obtain a best-fit film thickness. The best-fit value was found to

be dp/60. This value was used to predict effluent concentration histories for Li^+/Na^+ exchange and K^+/Li^+ exchange. In both cases, the histories were accurately predicted. The predicted effluent concentration histories for Li^+/Na^+ exchange is shown in Figure 8.

In conclusion, experimental studies indicate the coherence technique provides a good description of fixed-bed ion-exchange behavior. The coherence theory correctly identifies the location of transition and plateau zones for simple single abrupt influent changes, as well as for more complex multiple abrupt changes generating interferences within the column and for linear influent changes which generate a noncoherent zone. Generally, the predicted plateau compositions were accurate to well within the experimental error in the measuring technique ($\pm$ 4%). The kinetic limitations of the theory are reflected in that actual boundaries are more diffuse than predicted boundaries and actual peak compositions are smaller than predicted. Experimental studies of binary exchange systems indicate that the non-equilibrium model provides an accurate description of column behavior provided an appropriate expression for particle film thickness is used. Further work is necessary in order to establish a correlation for the estimation of film thickness.

NOMENCLATURE

a_{ij}	Stefan-Maxwell coefficient
a_p	effective interface area per unit volume contacting system
c_i	concentration of species i in fluid per unit volume of bed
$\bar{c}_i$	concentration of species i in resin per unit volume of bed
c	total concentration of exchanging species in fluid per unit volume of bed
$\bar{c}$	total concentration of exchanging species in resin per unit volume of bed
$\hat{c}$	total concentration of exchanging species per unit volume of resin
dp	diameter of ion-exchange particle
F	volumetric flow rate
f	Faraday's gas constant

g_{ij} binary constant
h h root
h_i ith h root
J_i diffusional flux of species i
k Boltzmann constant
n unit vector normal to resin surface
R gas constant
R_i generalized rate function
t time
T absolute temperature
u adjusted concentration velocity
u_{x_i} adjusted liquid concentration velocity of species i
u_{y_i} adjusted resin concentration velocity of species i
u_o linear approach velocity
v concentration velocity
v_{c_i} concentration velocity of species i
v_{h_i} h root velocity
V solution volume in time t
x_i fraction of species i in the mobile phase
y_i fraction of species i in the resin phase
$\bar{y}_i$ fraction of species i in the resin phase (all species including solvent and fixed site)
$\bar{y}_{ij}$ effective mole fraction of species i and j in resin phase (all species including solvent and fixed site)
z distance from column inlet
z_i valency of ionic species

Greek Symbols

α_{ij} separation factors of species i and j
δ film thickness
ε column void fraction
ε_p fractional pore volume of ion exchanger
η viscosity of solution
θ volumetric throughput parameter

μ	chemical potential
μ'	electrochemical potential
υ	bed volume
τ	adjusted time
T	tortuousity factor
ϕ	electrical potential
ω_i	ionic mobility of species i

Superscripts

o	refers to infinite dilution
*	refers to equilibrium conditions

Subscripts

f	refers to fixed ionic site in resin
i	refers to species i
I	evaluated at the interface
j	refers to species j
s	refers to free solvent

REFERENCES

1. Vermeulen, T., G. Klein and N. K. Hiester, in Chemical Engineer's Handbook, 5th Edition, Section 16, R. H. Perry and C. H. Chilton, eds., McGraw-Hill, New York (1973).

2. Helfferich, F. and G. Klein, Multicomponent Chromatography, Marcel Decker, New York, (1970).

3. Frenz, J. and C. Horvath, AIChE J., 31, 400 (1985).

4. Helfferich, F. and D. B. James, J. Chromatogr., 46, 1 (1970).

5. Clifford, D., Ind. Eng. Chem. Fundam., 21, 141 (1982).

6. Wang, N. L., and S. Huang, AIChE Symposium Series, Adsorption and Ion Exchange, 79, 26 (1983).

7. Tien, C., J. S. Hsieh, and R. M. Turian, AIChE J., 22, 498, (1976).

8. Bailly, M. and D. Tondeur, Chem. Eng. Sci., 36, 455 (1981).

9. Davis, M. M. and M. D. LeVan, AIChE J., 33, 470 (1987).

10. Nervick, W. E., J. Phys. Chem., 59, 690 (1955).

11. DeVault, D., J. Amer. Chem. Soc., 65, 532 (1943).

12. Pinto, N. G. and E. E. Graham, AIChE J., 32, 291 (1986).

13. Van Brakel, J. and P. M. Heertjes, Int. J. Heat Mass Transfer, 17, 1093 (1974).

14. Glueckauf, E. and J. I. Coates, J. Chem. Soc., 1947, 1315 (1955).

15. Scatchard, G. and N. J. Anderson, J. Phys. Chem., 58, 596 (1954).

16. Pinto, N. G. and E. E. Graham, Ind. Eng. Chem. Research, in 26, 2331 (1987).